

Interacting semi-flexible self-avoiding walks studied on a fractal lattice

Duška Marčetić

University of Banja Luka, Faculty of Natural Sciences and Mathematics,
M. Stojanovića 2, 78 000 Banja Luka, Bosnia and Herzegovina

E-mail: dusanka.marcetic@pmf.unibl.org

Abstract. Self-avoiding walks are studied on the 3-simplex fractal lattice as a model of linear polymer conformations in a dilute, non-homogeneous solution. A model is supplemented with bending energies and attractive-interaction energies between non-consecutively visited pairs of nearest-neighboring sites (contacts). It captures the main features of a semi-flexible polymer subjected to variable solvent conditions. Hierarchical structure of the fractal lattice enabled determination of the exact recurrence equations for the generating function, through which universal and local properties of the model were studied. Analysis of the recurrence equations showed that for all finite values of the considered energies and non-zero temperatures, polymer resides in an expanded phase. Critical exponents of the expanded phase are universal and the same as those for ordinary self-avoiding walks on the same lattice found earlier. As a measure of local properties, the mean number of contacts per mean number of steps as well as persistence length, are calculated as functions of Boltzmann weights associated with bending energies and attractive interactions between contacts. Both quantities are monotonic functions of stiffness weights for fixed interaction, and in the limit of infinite stiffness the number of contacts decreases to zero, while the persistence length increases unboundedly.

Keywords: Self-avoiding walks; Interaction; Stiffness; Fractal; Generating functions

1. Introduction

A self-avoiding walk (SAW) on a lattice is a sequence of consecutive steps along the lattice bonds in which the steps are not allowed to go through the same lattice site more than once [1]. Due to their vast range of applications in different areas, but most commonly in polymer related problems [2,3], SAWs have become subject of continuous research interest since their introduction [4,5]. They belong to the class of combinatorial concepts which are simple to state but difficult or even impossible to solve exactly. In polymer physics, SAWs are canonical lattice model for conformations of a single linear polymer dissolved in a good solvent. Non-intersecting property of SAWs corresponds to an excluded volume effect of a polymer, and that is the only interaction relevant in a good solvent conditions, i.e. at high temperatures. More realistic model that captures the behavior of a polymer at all solvent temperatures can be obtained by implementing ordinary SAWs with an attractive interaction between contacts, i.e. visited pairs of sites that are nearest-neighbors but not adjacent along the walk. Such an interaction represents monomer-monomer interaction mediated by the solvent and thus mimics different solvent qualities. Many aspects of the interacting model have been intensively studied concerning the polymer collapse transition [6–23]. Another step that improves the model is the addition of bending energy to each bend in the walk so that various degrees of stiffness of natural polymers could be accounted for. Influence of stiffness on the polymer collapse and phase diagram in general has also been considered on regular lattices [24–28]. In all of these studies it is assumed that the polymer is immersed in a homogeneous solution. However, in many real situations that might not be the case if some impurities or obstacles are dispersed in solution. Presence of disorder can affect the critical properties of polymers modelled by the SAWs [29,30]. In order to study its impact, disordered environment is usually represented by translationally non-invariant lattices such as randomly diluted and fractal lattices. Deterministic fractals have an advantage of being scale invariant, a symmetry that allows for many exactly solved problems by the application of an exact recursive method. Critical behavior of self-avoiding walks with contact interactions or bending stiffness on fractal lattices are studied in [31–37]. Despite aforementioned advantage of fractal lattices, SAWs with both, interaction and stiffness, require in their recursive treatment a large number of variables even on the simplest fractal lattice. Therefore, to the best of our knowledge, there is only one such study [38], where the phase diagram on the 4-simplex lattice is obtained by the renormalization group approach.

In the present paper, we have considered self-avoiding walks with contact interactions and bending stiffness (Interacting semi-flexible self-avoiding walk model, ISFSAW) on the fractal, 3-simplex lattice. Critical behaviour of the reduced models: Interacting self-avoiding walks (ISAW) [32], Semi-flexible self-avoiding walks (SFSAW) [37] and ordinary Self-avoiding walks (SAW) [39] have already been studied on this lattice with the focus on critical exponents. Here we found that global behavior of the compound model is almost the same as the behavior of the reduced models, since all

finite values of the interaction parameters describe a polymer in an expanded phase. At zero temperature, flexible polymer is in a compact phase, while semi-flexible polymer is in a rigid-rod phase. Furthermore, we have studied nonuniversal properties of the model. In the framework of the grand canonical ensemble, we have determined critical fugacity surface and studied the influence of bending and interaction energies on the structure of conformations by calculating the mean number of contacts per mean number of steps and persistence length. In section 2, we describe the model, outline a method in general and apply it on the 3-simplex lattice. Analysis of the recurrence equations and calculation procedure are presented in section 3, while results and discussion are presented in subsection 3.1 for flexible and subsection 3.2 for semi-flexible walks. Summary of the paper and conclusions are presented in section 4. Appendix A contains a complete set of recurrence equations complementing the generating function of open walks.

2. A model and grand canonical formalism on the 3-simplex lattice

The 3-simplex lattice is a finitely ramified fractal lattice introduced by Dhar [39,40]. The lattice is similar to the Sierpinski gasket and has the same fractal dimension $d_f = \frac{\ln 3}{\ln 2}$, but is less demanding regarding the number of variables and their equations in studying SAW lattice problems [41]. Lattice construction follows the iterative steps, where prefractal structure obtained in the r -th step is called the r -th order generator ($G^{(r)}$), and the whole lattice is obtained by letting $r \rightarrow \infty$. The third order generator is shown in Figure 1 altogether with one self-avoiding walk consisting of $N = 19$ steps. In the ISFSAW model each polymer conformation is represented by the weighted walk on a lattice: Boltzmann factors $u = \exp(-\epsilon/kT)$ and $s = \exp(-\epsilon_b/kT)$ are associated with each contact and each bend of the walk, respectively. These factors are illustrated along with the walk shown in Figure 1. Interactions that we consider here are restricted to $-\infty \leq \epsilon \leq 0$ and $0 \leq \epsilon_b \leq \infty$, but these sets can be extended to include super-perfect solvent ($\epsilon > 0$) [7] and super-flexible walks $\epsilon_b < 0$ [42, 43]. Energy of an N -step walk with M contacts and N_b bends is $E_N(M, N_b) = M\epsilon + N_b\epsilon_b$, so that canonical partition function is $Z_N = \sum_{N_b} \sum_M W_N(N_b, M) s^{N_b} u^M$, where $W_N(N_b, M)$ is the number of different N -step self-avoiding walks of energy $E_N(M, N_b)$, per lattice site. Assigning a fugacity x to each step of the walk, grand canonical partition function reads $\mathcal{G}(x, s, u) = \sum_{N=0}^{\infty} \sum_{N_b} \sum_M W_N(N_b, M) x^N s^{N_b} u^M$. It is an overall weight of all possible walks, and the weight $x^{19} s^{14} u^6$ of the walk shown in Figure 1 is just one term in \mathcal{G} . Grand canonical partition function is the generating function for the sequence Z_N and can also be written as $\mathcal{G} = \sum_{N=0}^{\infty} x^N Z_N$. It is assumed that the leading order behaviour of Z_N is $Z_N \sim \omega(s, u)^N$ in the limit $N \rightarrow \infty$, so that the radius of convergence of \mathcal{G} is given by $x_c(s, u) = (\omega(s, u))^{-1}$. For $x < x_c$ the mean length $\langle N \rangle$ of walks is finite, whereas for $x \geq x_c$ it diverges. The so called polymerization transition, which occurs at critical fugacity x_c , corresponds to the thermodynamic limit. Free energy per step in the thermodynamic limit, defined as $f = -k_B T \lim_{N \rightarrow \infty} (\ln Z_N / N)$, is then given by $f = -k_B T \ln \omega(u, s) = k_B T \ln x_c(u, s)$, from which all thermal, bulk properties of

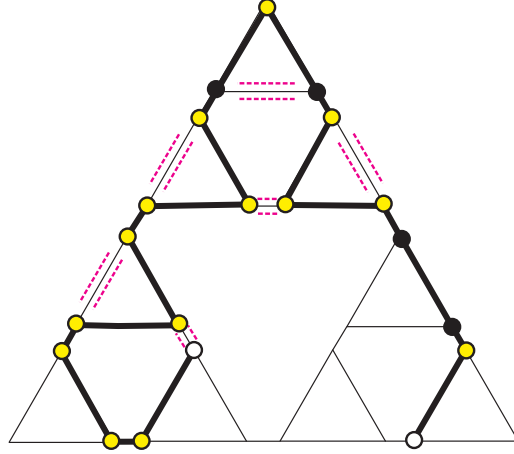


Figure 1. A self-avoiding walk consisting of $N = 19$ steps on the third order generator of the 3-simplex lattice. Lattice sites visited by the walk are represented with circles in different colors, where white circles represent sites with the endpoints of the walk. At each yellow site the walk makes a bend to which a Boltzmann factor s is assigned. Attractive interactions between contacts are marked with the double dashed lines and weighted with the factors u . Finally, each step of the walk is weighted with a fugacity x , so that the total weight of the walk is $x^{19}s^{14}u^6$.

the system can be found. Here, it is more convenient to work in the grand canonical formalism, where the mean number of steps, contacts and bends are given by

$$\langle N \rangle = \frac{1}{\mathcal{G}} \sum_{N,M,N_b} N W_N(N_b, M) x^N s^{N_b} u^M = \frac{x}{\mathcal{G}} \frac{\partial \mathcal{G}}{\partial x}, \quad (2.1)$$

$$\langle M \rangle = \frac{1}{\mathcal{G}} \sum_{N,M,N_b} M W_N(N_b, M) x^N s^{N_b} u^M = \frac{u}{\mathcal{G}} \frac{\partial \mathcal{G}}{\partial u}, \quad (2.2)$$

$$\langle N_b \rangle = \frac{1}{\mathcal{G}} \sum_{N,M,N_b} N_b W_N(N_b, M) x^N s^{N_b} u^M = \frac{s}{\mathcal{G}} \frac{\partial \mathcal{G}}{\partial s}. \quad (2.3)$$

Quantities of interest: the mean number of contacts and the mean number of bends per mean number of steps, are

$$m = \frac{\langle M \rangle}{\langle N \rangle} = \frac{u}{x} \frac{\mathcal{G}^u}{\mathcal{G}^x} \quad \text{and} \quad n_b = \frac{\langle N_b \rangle}{\langle N \rangle} = \frac{s}{x} \frac{\mathcal{G}^s}{\mathcal{G}^x}, \quad (2.4)$$

where $\mathcal{G}^x = \left(\frac{\partial \mathcal{G}}{\partial x} \right)_{u,s}$, $\mathcal{G}^u = \left(\frac{\partial \mathcal{G}}{\partial u} \right)_{x,s}$ and $\mathcal{G}^s = \left(\frac{\partial \mathcal{G}}{\partial s} \right)_{x,u}$. All partial derivatives should be calculated at the critical value $x_c(u, s)$. A measure of polymer persistency obtained as $l_p = \langle N \rangle / \langle N_b \rangle = 1/n_b$, has the meaning of an average number of steps between two consecutive bends (average length of straight segments) and will be considered as a persistence length throughout this paper.

In order to construct $\mathcal{G}(x, s, u)$ for the ISFSAW model on the 3-simplex lattice, one finds that twenty restricted generating functions are involved, but it turned out that only six of them are actually strictly necessary. These six restricted generating

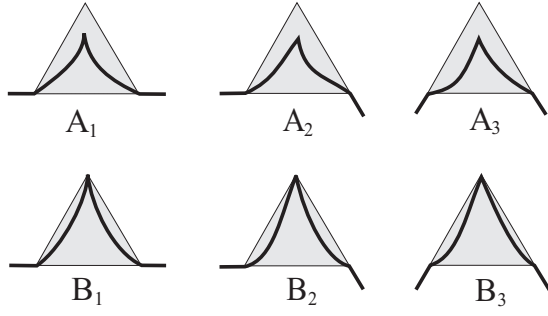


Figure 2. Restricted generating functions necessary for recursive formulation of the ISFSAW model on the 3-simplex lattice. They are classified according to the number of visited corner vertices (A and B) and directions of the first steps external to the generator (1, 2 and 3). Also, $A_i \supset B_i$ for $i = 1, 2, 3$.

functions are the weights of the corresponding SAWs, denoted as A_1 , A_2 , A_3 , B_1 , B_2 and B_3 , which comprise self-avoiding polygons, or walks (open) with the endpoints fixed at the corner vertices of the largest generator. They are shown schematically in Figure 2. With A we denote all SAWs that enter a generator (of any order) at one corner vertex and leave it at another. A -type walks includes both: walks that visit the third corner vertex of a generator and those which do not visit it. In order to properly account for the interactions at all levels of the fractal structure, B -type of walks are introduced as those subset of walks A which obligatory visit the third corner vertex of the generator. With that set of variables, recurrence equations of the interacting model can be obtained from the equations for ordinary SAWs by subtracting some terms with weights B from weights A , and adding them properly with the interaction [32,39]. Further classification to A_i and B_i , $i = 1, 2, 3$, is made according to the direction of external steps with which walks enter and leave a generator, in order to include possible bends at its corner vertices. Following the illustration in Figure 3 from which the recurrence equation for variable A_1 is derived, all recurrence equations can be written as

$$A_{1r+1} = A_{1r}^2 + A_{2r}^2 A_{3r} + (u-1)A_{3r}B_{2r}^2, \quad (2.5a)$$

$$A_{2r+1} = A_{1r}A_{2r} + A_{1r}A_{2r}A_{3r} + (u-1)A_{3r}B_{1r}B_{2r}, \quad (2.5b)$$

$$A_{3r+1} = A_{2r}^2 + A_{1r}^2 A_{3r} + (u-1)A_{3r}B_{1r}^2, \quad (2.5c)$$

$$B_{1r+1} = A_{2r}^2 B_{3r} + (u-1)B_{2r}^2 B_{3r}, \quad (2.5d)$$

$$B_{2r+1} = A_{1r}A_{2r}B_{3r} + (u-1)B_{1r}B_{2r}B_{3r}, \quad (2.5e)$$

$$B_{3r+1} = A_{1r}^2 B_{3r} + (u-1)B_{1r}^2 B_{3r}. \quad (2.5f)$$

Initial values given on a unit triangle are: $A_{11} = x^2 + x^3 s^3 u$, $A_{21} = x^2 s + x^3 s^2 u$, $A_{31} = x^2 s^2 + x^3 s u$, $B_{11} = x^3 s^3 u$, $B_{21} = x^3 s^2 u$ and $B_{31} = x^3 s u$. Interaction and bending parameters vary over the intervals $[1, \infty]$ and $[0, 1]$, respectively. For $u = 1$ and $s = 1$, SAWs are non-interacting and flexible (ordinary SAWs). Smaller s corresponds to stiffer chain and $s \rightarrow 0$ is a rigid-rod limit.

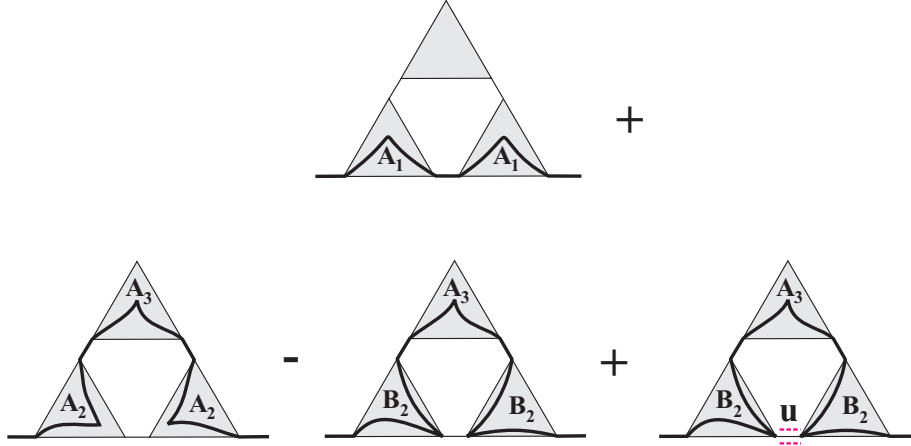


Figure 3. Schematic representation of the procedure with which recurrence equation (2.5a) is obtained. Larger triangle is a generator of order $r + 1$, while smaller, shaded triangles are the generators of the r -th order. The overall weight of the walk on the larger triangle is obtained by the multiplication of the weights assigned to the smaller constitutive triangles. Each such overall weight corresponds to one term in recurrence equation (2.5a). The third term is subtracted from the second and added multiplied by the factor u because an interaction between smaller triangles occurred.

3. Analysis of the model and calculation

Polygon generating function is given by

$$P(x, s, u) = \frac{1}{3}x^3s^3 + \sum_{r=1}^{\infty} \frac{1}{3^{r+1}} \left(A_{3r}(x, s, u) \right)^3, \quad (3.1)$$

and can also be written recurrently in the form $P_{r+1} = P_r + (A_{3r})^3/3^{r+1}$ with $P_1 = (1/3)x^3s^3$. Iterating (3.1) together with recurrence equations (2.5a)-(2.5f), for each particular pair of u and s , critical fugacity x_c is determined as the largest value of x at which the generating function P converges. Such a behaviour of P can be deduced from the behaviour of the reduced generating functions A_i and B_i , $i = 1, 2, 3$. Indeed, for every $x < x_c(s, u)$ all the variables A_i and B_i tend toward zero, while for $x > x_c(s, u)$ they diverge (and so does P). For $x = x_c(s, u)$ they tend to $A^*, A^*, A^*, 0, 0, 0$, with $A^* = 0.61803\dots$. This is the fixed point of the system of nonlinear difference equations (2.5a)-(2.5f), as can be checked. By putting $B_i^* = 0$ and $A_i = A^*$ for $i = 1, 2, 3$, the fixed point equation for variables A_i reduces to $A^* = A^{*2} + A^{*3}$ with the nontrivial solution $A^* = (\sqrt{5} - 1)/2 = 0.61803\dots$, the same as in [32, 37, 39]. This nontrivial fixed point corresponds to an expanded, swollen phase of a polymer, with the end-to-end critical exponent ν given by $\nu = \ln 2 / \ln(\frac{7-\sqrt{5}}{2}) \approx 0.7986$ [32, 39]. Thus, for all finite and non-zero values of the parameters u and s , polymer is in the expanded phase with constant critical exponent ν . There is no collapsed phase on the 3-simplex lattice for any finite u . Another nontrivial fixed point $(1, 0, 0, 0, 0, 0)$ of the system (2.5a)-(2.5f) can be reached for $s = 0$ and $x_c = 1$. It is an unstable fixed point that corresponds to a rigid-rod phase of a polymer, also found in [37]. In this phase polymer is fully elongated, with no

bends, and the end-to-end distance scales with the number of steps as $\mathcal{R} \sim N$, so that $\nu = 1$. Critical exponent ν can be obtained numerically by noticing that $\mathcal{R}_r \sim 2^r \sim N_r^\nu$, where \mathcal{R}_r is a root mean square end-to-end distance of a walk that occupies r -th order generator of linear size 2^r , and N_r is the number of steps of the walk. Writing similar expression that holds at the stage $r + 1$, it follows that $\nu = \ln(2)/(\ln N_{r+1}/\ln N_r)$. For all finite values of u and $s \neq 0$, we have numerically obtained $\nu \approx 0.7986$. When $s = 0$ then $x_c=1$ and $\nu = 1$ numerically, but it also follows from the previous expression for ν given that $N_r \sim 2^r$ in the rigid-rod phase.

Generating functions for polygons and open walks (\mathcal{G}) have the same radius of convergence x_c , but they behave differently at x_c . Namely, P converges at x_c while \mathcal{G} diverges. Moreover, the mean length of polygons (determined by the first derivative of P) stays finite at $x = x_c$ and is short, so that thermodynamic limit is not approached even after many iterations. Therefore, we have calculated the mean length $\langle N \rangle$ of open walks by using the generating function

$$\mathcal{G}(x, s, u) = x(1+xsu) + \sum_{r=1}^{\infty} \frac{1}{3^r} (C_r^2 + A_{3r}C_r^2 + (u-1)A_{3r}D_{1r}^2 + A_{3r}^2G_{3r}), \quad (3.2)$$

with which $\langle N \rangle$ diverges at x_c when the number of iterations tends toward ∞ . In \mathcal{G} , walks with one or both endpoints in the interior vertices are also contained. Their recurrence equations are given in Appendix A. But, as we have already mentioned, equations (2.5a)-(2.5f) suffice for the calculation of the mean values (2.4), since they can be calculated by using the corner-to-corner restricted generating function A_1 which behaviour at x_c is the same as of \mathcal{G} . We have checked that all quantities defined per step of the walk or per lattice site, calculated via A_1 , are the same as those calculated via \mathcal{G} . To calculate (2.1)-(2.4), we need all variables A_i and B_i , $i = 1, 2, 3$, and their first derivatives with respect to x , u and s . From recurrence equations (2.5a)-(2.5f) we see that $A_{i_{r+1}} = f_i(A_{j_r}(x, u, s), B_{j_r}(x, u, s), u)$ and $B_{i_{r+1}} = g_i(A_{j_r}(x, u, s), B_{j_r}(x, u, s), u)$, where f_i and g_i are some polynomial functions and $i, j = 1, 2, 3$. With variables that denote partial derivatives with respect to x holding u and s constant: $A_{i_{r+1}}^x = \frac{\partial A_{i_{r+1}}}{\partial x}$, $B_{i_{r+1}}^x = \frac{\partial B_{i_{r+1}}}{\partial x}$, $A_{i_r}^x = \frac{\partial A_{i_r}}{\partial x}$ and $B_{i_r}^x = \frac{\partial B_{i_r}}{\partial x}$, recurrence equations for partial derivatives can be written in the form of a matrix equation, where 6×6 matrix connects two columns of order 6×1 :

$$\begin{pmatrix} A_{i_{r+1}}^x \\ B_{i_{r+1}}^x \end{pmatrix} = \begin{pmatrix} \frac{\partial f_i}{\partial A_{j_r}} & \frac{\partial f_i}{\partial B_{j_r}} \\ \frac{\partial g_i}{\partial A_{j_r}} & \frac{\partial g_i}{\partial B_{j_r}} \end{pmatrix} \begin{pmatrix} A_{j_r}^x \\ B_{j_r}^x \end{pmatrix} \quad i, j=1, 2, 3. \quad (3.3)$$

Initial conditions are obtained from the corresponding initial conditions for variables A_i and B_i , and are given by $A_{11}^x = 2x + 3x^2s^3u$, $A_{21}^x = 2xs + 3x^2s^2u$, $A_{31}^x = 2xs^2 + 3x^2su$, $B_{11}^x = 3x^2s^3u$, $B_{21}^x = 3x^2s^2u$ and $B_{31}^x = 3x^2su$. In a similar manner we obtained recurrence equations for partial derivatives with respect to s and u . Thus, for each s , u and $x_c(s, u)$, six original and eighteen additional recurrence equations (for first derivatives) were iterated, and quantities (2.1)-(2.4) calculated. One should mention that all results obtained for m and l_p that we present in the next subsections should hold equally well for walks and polygons, since both types of walks have the same

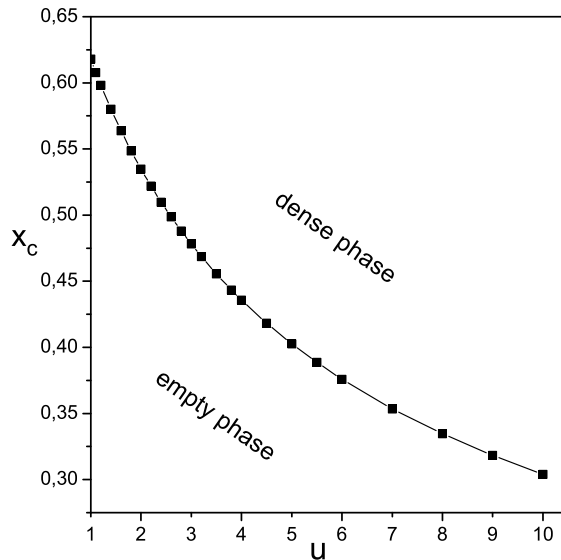


Figure 4. Dependence of critical fugacity x_c on the interaction parameter u for $s = 1$. Above the critical line, the phase is polymerized with the finite density of monomers (dense), whereas below the critical line it is unpolymerized with zero density (empty). At the critical line, the phase is the polymerized, expanded with zero density.

growth constant $\omega(s, u) = 1/x_c(s, u)$ and thus the free energy in the thermodynamic limit. Equality of m for walks and polygons has been deduced and numerically confirmed on regular lattices as well [18, 19].

3.1. Results and discussion, $s = 1$

In this subsection we present results for critical fugacity, density of monomers, m and l_p for flexible interacting walks ($s = 1$, $1 \leq u \leq \infty$).

In Figure 4, critical fugacity x_c is shown as a function of the interaction parameter u . For $x \geq x_c$, that is on the critical line and above it, the phase is polymerized with $\langle N \rangle = \infty$, whereas below the critical line the phase is unpolymerized with $\langle N \rangle = \text{const.}$ A polymerized phase on the critical line is the expanded phase for each value of u . As one can see, critical fugacity monotonically decreases with the interaction parameter u . When $u \rightarrow \infty$ ($\epsilon \rightarrow -\infty$ or $T \rightarrow 0$), it is found that $x_c \rightarrow 0$ and SAWs become maximally compact. It is not difficult to see that the growth constant of the maximally compact SAWs, μ_C , can be deduced from the critical fugacity in the $u \rightarrow \infty$ limit. For flexible SAWs, $\mathcal{G}(x, u) = \sum_N x^N Z_N(u)$ where $Z_N(u) = \sum_M C_N(M) u^M$ is canonical partition function. When $u \rightarrow \infty$, Z_N is dominated by the term with the maximal number of contacts, that is, $Z_N \approx u^{M_{max}} C_N(M_{max})$ with $M_{max} = \frac{1}{2}(q-2)N$ being the maximal number of contacts on a lattice with the coordination number q . If we assume that the number of maximally compact SAWs, $C_N(M_{max})$, asymptotically grows as $(\mu_C)^N$, then the radius of convergency of \mathcal{G} is given by $x_c = \left(u^{\frac{q-2}{2}} \mu_C \right)^{-1}$. For 3-simplex lattice

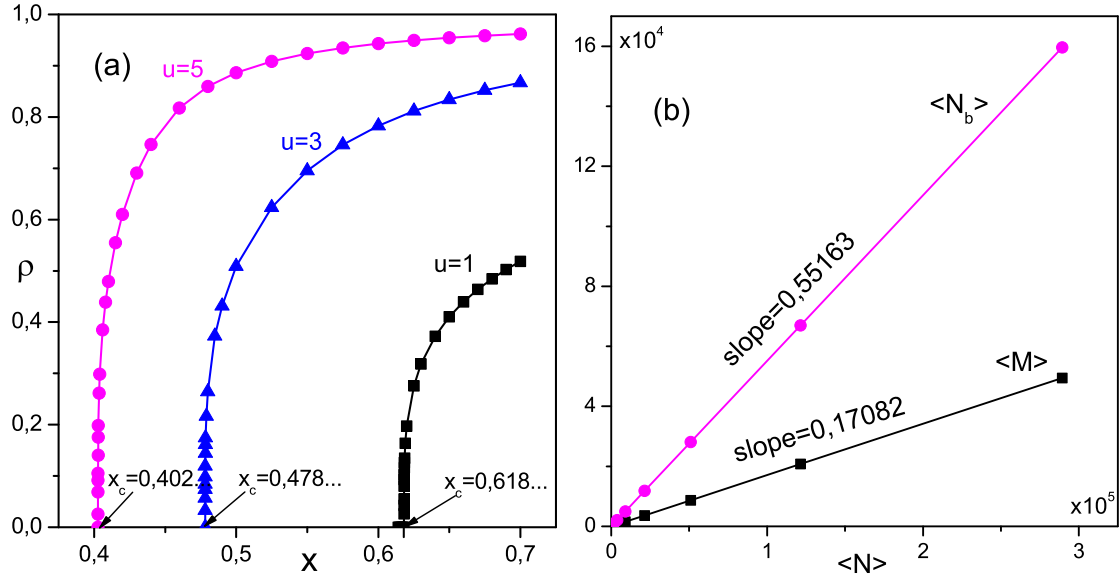


Figure 5. (a) Density of monomers as a function of fugacity x for fixed values of u . (b) Asymptotic proportionality of the mean number of contacts and bends to the mean number of steps for $u = 1$ and $s = 1$. The slopes m and n_b of the lines are shown with each graph.

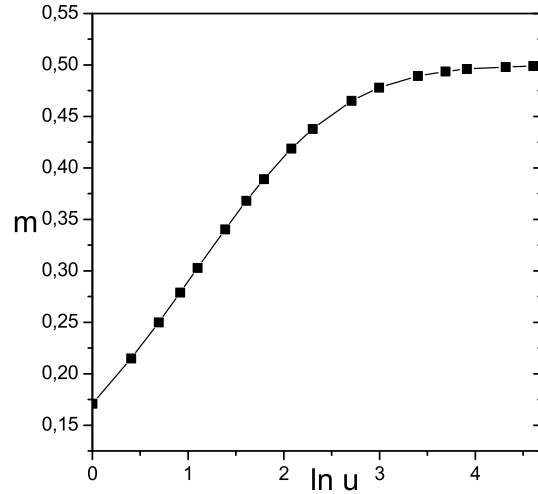


Figure 6. Mean number of contacts per mean number of steps as a function of $\ln(u)$.

$q = 3$ so that $\mu_C = \left(\sqrt{u} x_c\right)^{-1}$. Here we find $\mu_C \approx 0.998$ for $u = 50$ and $x_c = 0.14111\dots$, for example. For larger u , calculated values of μ_C tend toward 1, which is the exact value of the growth constant of Hamiltonian walks (HWs) on the 3-simplex lattice [44]. Hamiltonian walks have the same 'bulk' properties as the maximally compact SAWs. However, there might be some subtle differences regarding the surface effects on regular lattices that are still a matter of debate [45–49]. On fractal lattices, this subject is much more complicated [50, 51].

The average density of monomers is defined as a fraction of the r -th order

generator's sites occupied by the polymer, $\rho_r = \langle N_r \rangle / 3^r$. This quantity is nonzero in the polymerized phase above the critical line (hence it is called 'dense' as marked in Figure 4), whereas it is zero in the unpolymerized phase ('empty'). Density disappears continuously by crossing the critical line from above at $u < u_\theta$, as found on regular [20] and fractal lattice [35] when the critical line is crossed above the θ temperature. In Figure 5(a), we show the dependence of density on fugacity for three given values of u . One can see how density continuously vanishes at the critical fugacity for every u . When $x \rightarrow \infty$ then $\rho \rightarrow 1$, which means that all sites of the lattice are occupied, that is, SAWs become Hamiltonian walks. This limit is approached faster for larger values of u , as can be seen in Figure 5(a).

We now turn to the mean number of contacts and bends. We have established linear relationships $\langle M \rangle \sim m \langle N \rangle$ and $\langle N_b \rangle \sim n_b \langle N \rangle$ when $N \rightarrow \infty$, which is displayed in Figure 5(b) for $u = 1$ and $s = 1$. The same asymptotic behaviour of the mean number of contacts is also found on regular lattices [7–10]. Asymptotic ratio m is shown in Figure 6 as a function of $\ln u$. For smaller u this dependence is almost linear (so that m is a linear function of ϵ), similarly as on regular lattices [9, 14]. As u increases towards ∞ , m asymptotically reaches a maximal value $m_{max} = (q - 2)/2 = 0.5$, which it can have on the 3-simplex lattice.

3.2. Results and discussion, $0 < s \leq 1$

In this subsection we generalize results obtained for x_c , m and l_p on the case of semi-flexible interacting walks. By varying s over the interval $(0, 1]$ we obtain a critical surface shown in Figure 7 (left panel). For each s and u on the critical surface polymer is in the expanded phase. Dependence of x_c on s for fixed values of u is shown on the right-hand side panel. For fixed u , x_c is a monotonically decreasing function of stiffness parameter (increasing function of stiffness energy). As s decreases from 1, x_c increases and tends toward 1 when $s \rightarrow 0$, for each u .

Linear relationships $\langle M \rangle \sim m \langle N \rangle$ and $\langle N_b \rangle \sim n_b \langle N \rangle$ in the limit $N \rightarrow \infty$ are established for all values of s . In Figure 8, $m(s, u)$ is presented as a surface in three-dimensional space (left panel) and $m(s)$ for fixed values of u (right panel). One can see that m is a monotonically increasing function of interaction energy and decreasing function of stiffness energy. When $u \rightarrow \infty$ ($\epsilon \rightarrow -\infty$) semi-flexible walks become maximally compact as do flexible, although for smaller s (stiffer walks) this limit is approached much slower. But, when $s \rightarrow 0$, SAWs tend to a rigid-rod limit with $m = 0$ irrespectively of u . Analysing our numerical results we have found that $m \approx us^3$ for small s . When $u = 1$ this relation starts to hold for $s \leq 0.01$, and Figure 9 displays how limit $m/s^3 \rightarrow 1$ is approached when s is decreased over two orders of magnitude. Validity of relation has been checked numerically for s as small as 10^{-5} .

In Figure 10 (left panel), n_b is displayed as a function of s for fixed u , where it can be seen that the mean number of bends per mean number of steps monotonically decreases with stiffness energy. In the right panel of Figure 10, $l_p(s)$ for constant u is shown on

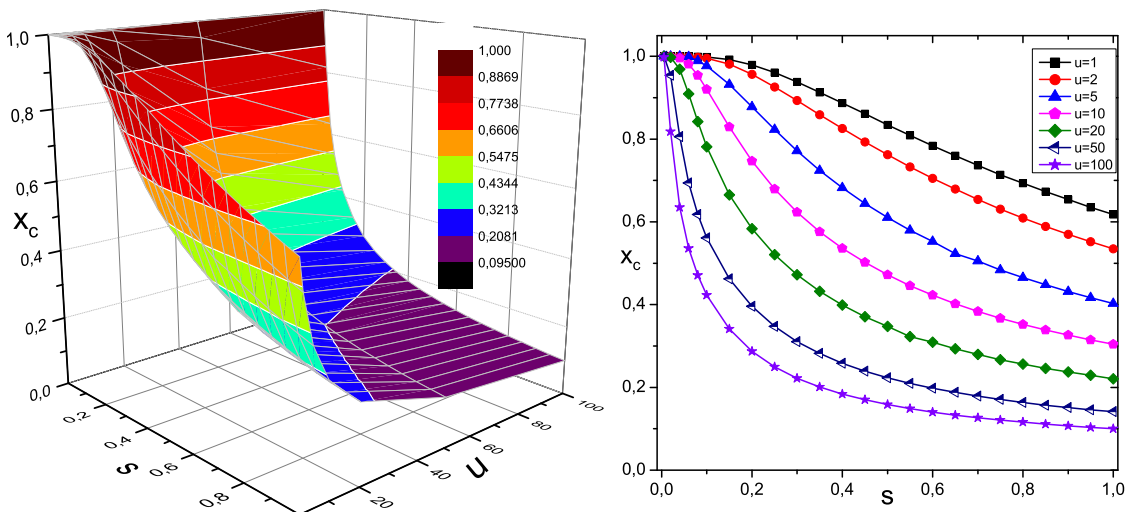


Figure 7. Critical fugacity surface (left panel) and constant u cross-sections (right panel).

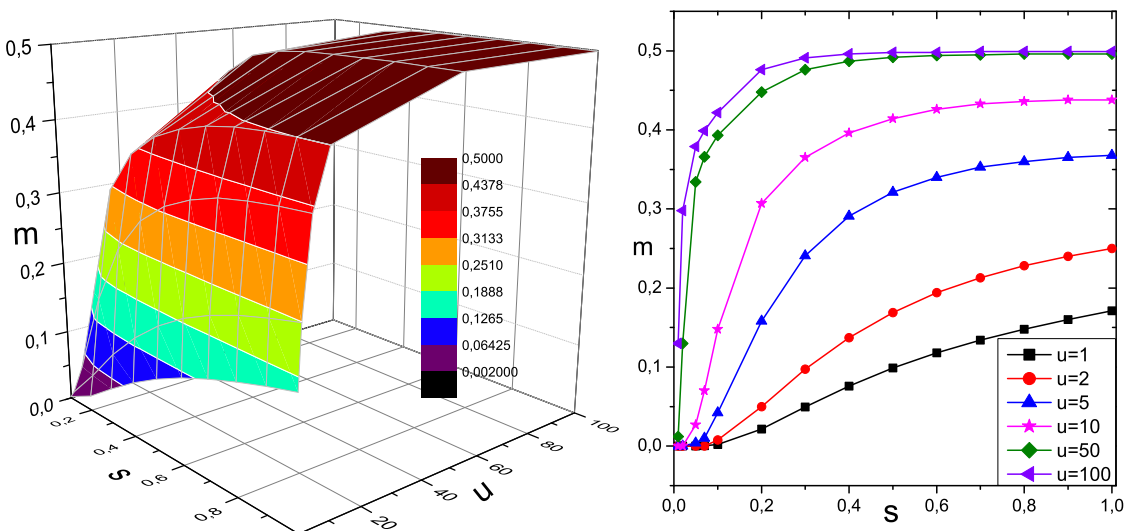


Figure 8. Mean number of contacts per mean number of steps as a function of parameters u and s (left panel). Constant u cross-sections (right panel).

the logarithmic scale in order to capture its fast growth for $s < 0.1$. One can see that the interaction delays this growth, but eventually all curves will terminate at infinity as $s \rightarrow 0$. We have found that the persistence length diverges as $l_p \sim 1/(3us^3)$ when $s \rightarrow 0$. However, much faster divergency, although of differently defined persistence length, was found in [37] on the same lattice. There, by applying scaling analysis on semi-flexible SAWs, it is concluded that persistence length should diverge as an exponential function of $1/s$ when $s \rightarrow 0$. In our numerical approach we first calculate critical fugacity x_c (exact x_c is known only for $s = 1$ and $u = 1$), so we deal with a value which is always slightly less than exact. We can achieve very high accuracy, for example, $x_c = 0.99999896840479804\dots$ is calculated with more than seventy significant

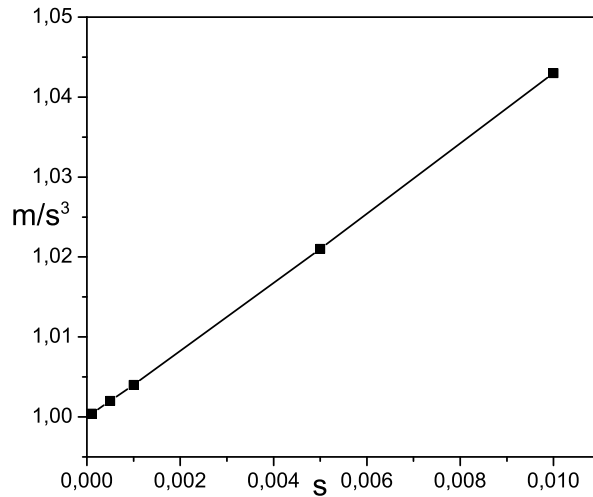


Figure 9. Ratio m/s^3 against s for $10^{-4} \leq s \leq 10^{-2}$.

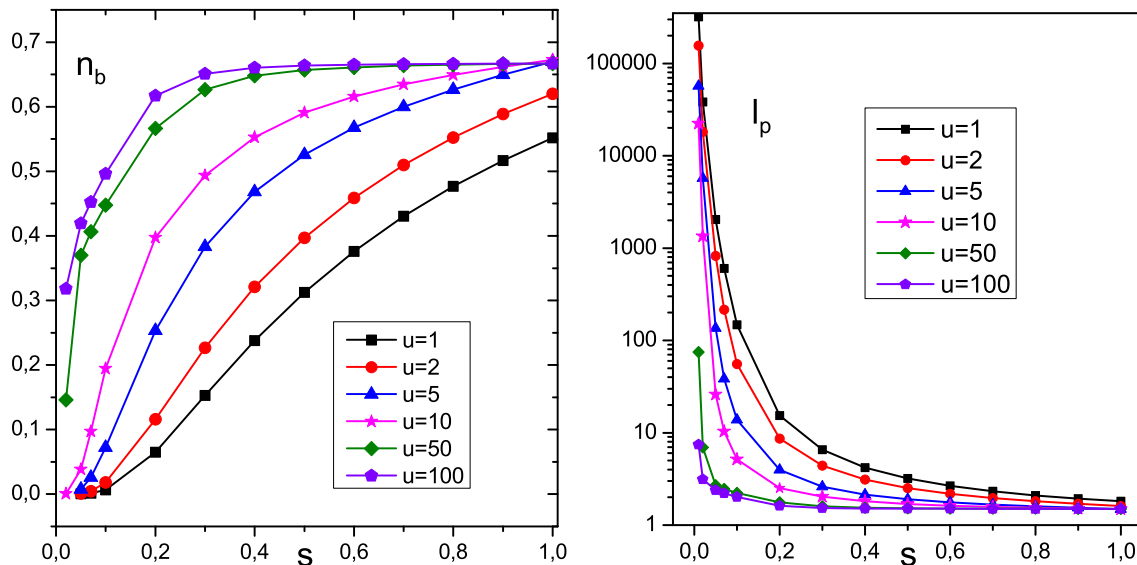


Figure 10. Mean number of bends per mean number of steps, n_b , as a function of s for fixed values of u (left panel). Persistence length $l_p = 1/n_b$ as a function of s for fixed values of u (right panel).

figures for $s = 0.01$, and we can perform very large number of iterations, which is all quite straightforward with a software like Maple. In such a way, we have found that although variables show crossover behaviour with the iterations, calculated quantities defined as ratios, do not. The flow of variables is exactly as was reasoned in [37]. Variable A_1 (which contains walks composed of straight steps) stays close to its initial value x_c^2 (just below 1) for the first hundred iterations, after which it moves toward fixed point A^* , where it stays nearby for almost next hundred iterations. Then it iterates to zero (a value that it has at the trivial attractive fixed point that governs the empty phase). Other variables, starting with their initial values, follow the similar trajectories. This complicated behaviour is reflected on the flow of the mean number of steps and

bends (as well as exponent ν), but not on the ratio $\langle N \rangle / \langle N_b \rangle$, which shows simple and fast convergency with the iterations. Thus, we think that persistence length considered in [37] and our l_p are different measures of persistency.

Some of the calculated values for m and l_p are presented in Table 1 and Table 2, respectively. From Table 1 we see that $m \approx 0.17082$ for ordinary SAWs, and we would like to compare it with the known values on regular lattices, since, to the best of our knowledge, there are no reported results on fractal ones. On hypercubic lattices with the coordination number $q = 2d$ in d -dimensional space $m \approx 0.1592(8), 0.201(1)$ and $0.174(2)$ for $d = 2, 3$ and 4 , respectively, thus largest in $d = 3$, as shown in [10]. Somewhat later result $0.17088(5)$ for $d = 4$ is reported in [52]. Beside dimension, on regular lattices m strongly depends on the lattice structure. In the same dimension m is larger on a lattice with larger coordination number, but it diminishes with dimension for the same coordination number. For the later example, m is much smaller on the tetrahedral lattice ($d = 3, q = 4$) than on the square lattice ($d = 2, q = 4$) [8]. However, minimal number of steps needed to make a contact ('minimum contact length' [10]), on the tetrahedral (diamond) lattice is large, it is 5 in comparison with 3 on the square lattice. One can expect that the interplay between lattice dimension and other properties of fractal lattices should influence m even in a more complicated manner. Coordination number of the 3-simplex lattice is 3, its fractal dimension is $d_f \approx 1.58$ and embedding dimension is $d = 2$, but m exceeds the value on the square lattice. Again, the minimal contact length is just 2 which supports a larger m obtained. Regarding persistence length, it can be seen in Table 2 that l_p is slightly a non-monotonic function of u for $s = 1$. It is approximately 1.8128 for $u = 1$ and tends toward $\frac{3}{2}$ from below when $u \rightarrow \infty$. For semi-flexible SAWs, l_p also attains the limit $\frac{3}{2}$ when $u \rightarrow \infty$, albeit slower. In this limit SAWs become maximally compact and have the same l_p as Hamiltonian walks on the 3-simplex lattice [53]. Persistence length of semi-flexible HWs is independent of stiffness and equal to $\frac{3}{2}$ on 3-simplex lattice. On other fractal lattices, although stiffness dependent, l_p of semi-flexible HWs is finite even in the infinite stiffness limit [53, 54]. Since Hamiltonian walks visit all lattice sites and are enumerated on larger and larger lattices with boundaries always present, they are bounded by definition, which may reflect on l_p . Finally, one last note regarding persistence length. Values obtained here in the non-interacting case ($u = 1$) are larger than the values of equally defined l_p for semi-flexible SAWs on the square lattice [43], and for smaller s this discrepancy enlarges. This observation is in accord with the expectation that smaller space dimension should induce larger persistence length.

In the end, we would like to mention that the mean number of contacts per mean number of steps and persistence length are quantities that were suggested in [25] as the order parameters to monitor the freezing transition that the ISFSAW model displayed on the simple cubic lattice. It proved out here that these quantities together can reveal the local structure of the SAWs conformations characteristic for the expanded phase found for all nonzero temperatures. These conformations are coil-like with 'loops' of all sizes. To illustrate this point and quantify the loops, we recall that for ordinary SAWs

Table 1. Some numerical values for m , chosen from a large set of data calculated and used to produce graphs in Figure 8. Five significant figures are presented with the last digit rounded off.

m	$u = 1$	$u = 2$	$u = 5$	$u = 10$	$u = 100$
$s = 1$	0.17082	0.24998	0.36796	0.43830	0.49891
$s = 0.8$	0.14816	0.22805	0.36044	0.43641	0.49883
$s = 0.6$	0.11793	0.19369	0.34034	0.42575	0.49832
$s = 0.4$	0.07589	0.13739	0.29057	0.39578	0.49592
$s = 0.2$	0.021356	0.049914	0.15786	0.30744	0.47555
$s = 0.1$	0.0022517	0.0076104	0.04266	0.39168	0.42175
$s = 0.05$	0.00016400	0.00046479	0.0039838	0.02691	0.37853

Table 2. Values of l_p for some chosen u and s . Five significant figures are presented with the last digit rounded off.

l_p	$u = 1$	$u = 2$	$u = 5$	$u = 10$	$u = 100$
$s = 1$	1.8128	1.6133	1.4927	1.4856	1.4999
$s = 0.8$	2.0977	1.8109	1.5961	1.5403	1.5012
$s = 0.6$	2.6590	2.1789	1.7619	1.6236	1.5037
$s = 0.4$	4.2033	3.1162	2.1359	1.8086	1.5139
$s = 0.2$	15.381	8.6237	3.9493	2.5153	1.6214
$s = 0.1$	148.06	55.551	13.841	2.2337	2.0162
$s = 0.05$	2034.8	823.82	135.44	26.020	2.3861

$m \approx 0.1708$, so that there are approximately 6 steps per contact, which is the size of a loop. Also $n_b \approx 0.5516$, which means that there are about 3 bends in the loop. For large u loops are smaller and wigglier in the quasi zig-zag conformations. For small s loops are large, then both m and n_b tend toward zero, whereas $n_b/m \approx 3$ (for $s \neq 0$), which merely reflects a geometrical constraint of the 3-simplex lattice.

4. Summary and conclusions

In this paper we have studied interacting semi-flexible self-avoiding walks and polygons on the 3-simplex lattice, which can serve as a model of linear and ring polymer conformations in a nonhomogeneous environment. Analysis of the closed set of established recurrence equations has shown that for all non-zero values of the stiffness parameter s and finite values of the interaction parameter u , model describes a polymer in an expanded, swollen phase. By applying the grand canonical formalism, non-universal properties such as the mean number of contacts and the mean number of bends are calculated for the set of values satisfying $0 \leq u < \infty$ and $0 < s \leq 1$. Linear relationships $\langle M \rangle \sim m \langle N \rangle$ and $\langle N_b \rangle \sim n_b \langle N \rangle$ are established in the limit $N \rightarrow \infty$, and the ratios m and n_b are calculated numerically for various values of u and s . It is perceived that the calculated quantities should be valid equally well for self-avoiding

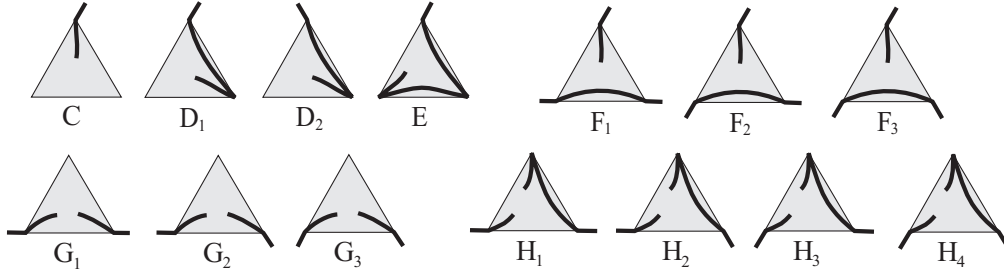


Figure A1. Walks with one or both endpoints in the interior vertices of the generator classified according to the number of visited corner vertices and direction of the first steps outside of the generator.

walks and polygons since the critical fugacity which determines free energy in the thermodynamic limit is the same for both types of walks. Results for m and $l_p = 1/n_b$ (which is a measure of polymer persistency) are presented and comprehensively discussed in subsections 3.1 and 3.2. Disorder modeled by the 3-simplex lattice brought about larger values of m and l_p obtained for ordinary SAWs in comparison with regular lattices. Interaction and stiffness energies influenced m and l_p independently, which resulted in monotonic behaviour. An exception is a slight non-monotonicity of l_p as a function of u for $s = 1$. Limiting values of parameters have also been considered. Semi-flexible SAWs in the limit $u \rightarrow \infty$ become maximally compact, with m and l_p that coincide with the results for Hamiltonian walks on the 3-simplex lattice. However, in the limit of infinite stiffness ($s \rightarrow 0$), stiffness completely prevails and conformations with the infinite persistence length, with no contacts, at $s = 0$ remain. We have found that in this limit the mean number of contacts per mean number of steps tends toward zero as $m \approx us^3$, while the persistence length diverges as $l_p \sim 1/(3us^3)$. At exactly $s = 0$ polymer is a rigid-rod. Since there have been no other results on this subject, it would be worthwhile to conduct a similar research on other fractal lattices to learn more about the influence of fractal space and interactions on these nonuniversal properties of SAWs.

Appendix A.

We supply additional types of walks that are involved in recursive formulation of the generating function (3.2). These are walks with one or both endpoints in the interior of the generator and are schematically presented in Figure A1. C is the weight of all SAWs that starts in the interior of the generator and leave it through one of the corner vertices with the external step along the fixed triangle side. These walks are symmetrically related with the walks directed along the other triangle side and thus have the same weight. They include walks that visit none, one and both of the remained corner vertices. Other walks are similarly defined. Some of them are supsets of others: $C \supset D_1 \supset E$, $G_1 \supset H_1$, $G_2 \supset H_2$, $G_3 \supset H_4$. Their recurrence equations are given by:

$$C' = C + (A_1 + A_2)C + (A_1 + A_2)A_3C + (F_1 + F_2)A_3^2 +$$

$$+ (u - 1)(B_1 + B_2)A_3D_1, \quad (\text{A.1})$$

$$D'_1 = A_2B_3C + (A_1A_3 + A_2)D_2 + (F_1 + F_2)A_3B_3 + \\ + (u - 1)(B_2B_3D_1 + A_3B_1E), \quad (\text{A.2})$$

$$D'_2 = A_1B_3C + (A_2A_3 + A_1)D_2 + (F_1 + F_2)A_3B_3 + \\ + (u - 1)(B_1B_3D_1 + A_3B_2E), \quad (\text{A.3})$$

$$E' = (A_1 + A_2)B_3D_2 + (F_1 + F_2)B_3^2 + (u - 1)(B_1 + B_2)B_3E, \quad (\text{A.4})$$

$$F'_1 = A_1^2C + A_2^2F_3 + A_1^2F_1 + A_1A_2F_1 + (u - 1)\left[(D_1 + D_2)A_1B_1\right. \\ \left.+ (B_1 + B_2)B_1F_1 + B_2^2F_3 + (u - 1)B_1^2E\right], \quad (\text{A.5})$$

$$F'_2 = A_1A_2C + A_1A_2F_3 + A_1^2F_2 + A_2^2F_1 + (u - 1)\left[A_1B_2D_2\right. \\ \left.+ A_2B_1D_1 + B_1B_2F_3 + B_1^2F_2 + B_2^2F_1 + (u - 1)B_1B_2E\right], \quad (\text{A.6})$$

$$F'_3 = A_2^2C + A_1^2F_3 + A_1A_2F_2 + A_2^2F_2 + (u - 1)\left[(D_1 + D_2)A_2B_2\right. \\ \left.+ (B_1F_3 + B_2F_2)B_1 + B_2^2F_2 + (u - 1)B_2^2E\right], \quad (\text{A.7})$$

$$G'_1 = C^2 + 2(F_1F_2 + F_1F_3 + F_2F_3)A_3 + 2A_2C^2 + 2(F_2 + F_3)A_1C \\ + (2A_3G_2 + A_2G_3)A_2 + 2A_1G_1 + (u - 1)\left[D_2^2 + 2A_2D_1^2\right. \\ \left.+ 2B_2CD_2 + 2(F_2 + F_3)B_1D_1 + 2(H_2 + H_3)A_3B_2 + B_2^2G_3 +\right. \\ \left.+ 2(u - 1)B_2D_1E\right], \quad (\text{A.8})$$

$$G'_2 = C^2 + 2(F_1 + F_2)A_3F_3 + (F_1^2 + F_2^2)A_3 + (A_1 + A_2)C^2 \\ + (A_1 + A_2)CF_3 + (A_1F_1 + A_2F_2)C + (A_1G_2 + A_2G_1)A_3 \\ + (A_2G_3 + G_2)A_1 + A_2G_1 + (u - 1)\left[A_1D_1^2 + (1 + A_2)D_1D_2\right. \\ \left.+ (B_2D_1 + B_1D_2)C + (B_1 + B_2)D_1F_3 + (B_1F_1 + B_2F_2)D_1\right. \\ \left.+ (H_2 + H_3)A_3B_1 + 2A_3B_2H_1 + B_1B_2G_3\right. \\ \left.+ (u - 1)(B_1 + B_2)D_1E\right], \quad (\text{A.9})$$

$$G'_3 = C^2 + 2(F_1F_2 + F_1F_3 + F_2F_3)A_3 + 2A_1C^2 + 2(F_1 + F_3)A_2C \\ + (2A_3G_1 + A_1G_3)A_1 + 2A_2G_2 + (u - 1)\left[D_1^2 + 2A_1D_1D_2\right. \\ \left.+ 2B_1CD_1 + 2(F_1 + F_3)B_2D_1 + 4A_3B_1H_1 + B_1^2G_3 +\right. \\ \left.+ 2(u - 1)B_1D_1E\right], \quad (\text{A.10})$$

$$H'_1 = A_2^2H_4 + (F_1F_2 + F_1F_3 + F_2F_3)B_3 + A_2CD_2 + (F_2 + F_3)A_1D_2 \\ + A_2B_3G_2 + (u - 1)\left[B_2^2H_4 + A_2D_1E + B_2D_2^2 + (F_2 + F_3)B_1E\right. \\ \left.+ (H_2 + H_3)B_2B_3 + (u - 1)B_2E^2\right], \quad (\text{A.11})$$

$$\begin{aligned}
H'_2 = & A_1 A_2 H_4 + (F_1 + F_2) B_3 F_3 + B_3 F_1^2 + A_1 C D_2 + (A_1 F_1 + A_2 F_3) D_2 \\
& + A_1 B_3 G_2 + (u - 1) \left[B_1 B_2 H_4 + A_1 D_1 E + B_1 D_2^2 \right. \\
& \left. + (B_1 F_1 + B_2 F_3) E + (H_2 + H_3) B_1 B_3 + (u - 1) B_1 E^2 \right], \quad (\text{A.12})
\end{aligned}$$

$$\begin{aligned}
H'_3 = & A_1 A_2 H_4 + (F_1 + F_2) B_3 F_3 + B_3 F_2^2 + A_2 C D_2 + (A_1 F_3 + A_2 F_2) D_2 \\
& + A_2 B_3 G_1 + (u - 1) \left[B_1 B_2 H_4 + A_2 D_2 E + B_2 D_1 D_2 \right. \\
& \left. + (B_1 F_3 + B_2 F_2) E + 2 B_2 B_3 H_1 + (u - 1) B_2 E^2 \right], \quad (\text{A.13})
\end{aligned}$$

$$\begin{aligned}
H'_4 = & A_1^2 H_4 + (F_1 F_2 + F_1 F_3 + F_2 F_3) B_3 + A_1 C D_2 + (F_1 + F_3) A_2 D_2 \\
& + A_1 B_3 G_1 + (u - 1) \left[B_1^2 H_4 + A_1 D_2 E + B_1 D_1 D_2 \right. \\
& \left. + (F_1 + F_3) B_2 E + 2 B_1 B_3 H_1 + (u - 1) B_1 E^2 \right]. \quad (\text{A.14})
\end{aligned}$$

Initial conditions are: $C(1) = x^{1/2}(1+x+xs+x^2su+x^2s^2u)$, $D_1(1) = x^{3/2}s(1+xsu+xu)$, $D_2(1) = x^{3/2}(1+xsu+xs^2u)$, $E(1) = x^{5/2}su(1+s)$, $F_1(1) = x^{5/2}u^2$, $F_2(1) = x^{5/2}su^2$, $F_3(1) = x^{5/2}s^2u^2$, $G_1(1) = xu(1+2xsu)$, $G_2(1) = xu(1+xu+xsu)$, $G_3(1) = xu(1+2xu)$, $H_1(1) = x^2su^2$, $H_2(1) = x^2u^2$, $H_3(1) = x^2su^2$ and $H_4(1) = x^2u^2$. On the unit triangle, fugacity x is assigned to each vertex through which the walk passes by and fugacity $x^{1/2}$ to each vertex which is a starting (ending) point of the walk, in order that each step of the whole walk gets proper fugacity x .

References

- [1] Madras N and Slade G 1993 *The Self-Avoiding walk* (Boston: Birkhäuser) p 435
- [2] Guttmann A J ed 2009 *Polygons, Polyominoes and Polycubes* (vol 775 Lecture notes in physics) (Berlin:Springer) p 499
- [3] Janse van Rensburg E J 2015 *The Statistical Mechanics of Interacting Walks, Polygons, Animals and Vesicles* (Oxford Lecture Series in Mathematics and Its Applications) (Oxford: Oxford University Press) p 625
- [4] Orr W J C 1947 Statistical treatment of polymer solutions at infinite dilution *Trans. Faraday Soc.* **43** 12–27
- [5] Flory P J 1949 The configuration of real polymer chains *J. Chem. Phys.* **17** 303–10
- [6] Ishinabe T 1985 Examination of the theta-point from exact enumeration of self-avoiding walks *J. Phys. A: Math. Gen.* **18** 3181–87
- [7] Fisher M E and Hiley B J 1961 Configuration and Free Energy of a Polymer Molecule with Solvent Interaction *J. Chem. Phys.* **34** 1253–67
- [8] Ishinabe T and Chikahisa Y 1986 Exact enumerations of self-avoiding lattice walks with different nearest-neighbor contacts *J. Chem. Phys.* **85** 1009–17
- [9] Ishinabe T 1987 Examination of the theta-point from exact enumeration of self-avoiding walks II *J. Phys. A: Math. Gen.* **20** 6435–53
- [10] Douglas J F and Ishinabe T 1995 Self-avoiding-walk contacts and random-walk self-intersections in variable dimensionality *Phys. Rev. E* **51** 1791–817
- [11] Derrida B and Saleur H 1985 Collapse of two-dimensional linear polymers: a transfer matrix calculation of the exponent ν_t *J. Phys. A: Math. Gen.* **18** 1075–79
- [12] Saleur H 1986 Collapse of two-dimensional linear polymers *J. Stat. Phys.* **45** 419–38
- [13] Binder P M, Owczarek A L, Veal A R and Yeomans J M 1990 Collapse transition in a simple polymer model: exact results *J. Phys. A: Math. Gen.* **23** L975–79

- [14] Nemirovsky A M, Dudowicz J and Freed K F 1992 Thermodynamics of a Dense Self-Avoiding Walk with Contact Interactions *J. Stat. Phys.* **67** 395–412
- [15] Grassberger P and Hegger R 1995 Simulations of three-dimensional θ polymers *J. Chem. Phys.* **102** 6881–89
- [16] Barkema G T and Flesia S 1996 Two-Dimensional Oriented Self-Avoiding Walks with Parallel Contacts *J. Stat. Phys.* **85** 363–81
- [17] Nidras P P 1996 Grand canonical simulations of the interacting self-avoiding walk model *J. Phys. A: Math. Gen.* **29** 7929–42
- [18] Tesi M C, Janse van Rensburg E J, Orlandini E and Whittington S G 1996 Interacting self-avoiding walks and polygons in three dimensions *J. Phys. A: Math. Gen.* **29** 2451–63
- [19] Bennett-Wood D, Enting I G, Gaunt D S, Guttmann A J, Leask J L, Owczarek A L and Whittington S G 1998 Exact enumeration study of free energies of interacting polygons and walks in two dimensions *J. Phys. A: Math. Gen.* **31** 4725–41
- [20] Foster D P and Seno F 2001 Two-dimensional self-avoiding walk with hydrogen-like bonding: phase diagram and critical behaviour *J. Phys. A: Math. Gen.* **34** 9939–57
- [21] Vogel T, Bachmann V and Janke W 2007 Freezing and collapse of flexible polymers on regular lattices in three dimensions *Phys. Rev. E* **76** 061803.
- [22] Ponmurugan M and Satyanarayana S V M 2012 The θ points of interacting self-avoiding walks and rings on a 2D square lattice *J. Stat. Mech.* P06010
- [23] Beaton N R, Guttmann A J and Jensen I 2020 Two-dimensional interacting self-avoiding walks: new estimates for critical temperatures and exponents *J. Phys. A: Math. Theor.* **53** 165002
- [24] Kolinski A, Skolnick J and Yaris R 1986 The collapse transition of semiflexible polymers. A Monte Carlo simulation of a model system *J. Chem. Phys.* **85** 3585–97
- [25] Bastolla U and Grassberger P 1997 Phase transitions of single semistiff polymer chains *J. Stat. Phys.* **89** 1061–78
- [26] Doye J P K, Sear R P and Frenkel D 1998 The effect of chain stiffness on the phase behaviour of isolated homopolymers *J. Chem. Phys.* **108** 2134–42
- [27] Lise S, Maritan A and Pelizzola A 1998 Bethe approximation for a semiflexible polymer chain *Phys. Rev. E* **58** R5241–44
- [28] Krawczyk A, Owczarek A L and Prellberg T 2009 Semi-flexible hydrogen-bonded and non-hydrogen bonded lattice polymers *Physica A* **388** 104–12
- [29] Chakrabarti B K ed 2005 *Statistics of Linear Polymers in Disordered Media* (Amsterdam: Elsevier) p 369
- [30] Bradley C J and Owczarek A L 2021 Effect of Lattice Inhomogeneity on Collapsed Phases of Semi-stiff ISAW Polymers *J. Stat. Phys.* **182** 27
- [31] Klein D J and Seitz W A 1984 Self-interacting self-avoiding walks on the Sierpinski gasket *J. Physique Lett.* **45** 241–47
- [32] Dhar D and Vannimenus J 1987 The collapse transition of linear polymers on fractal lattices *J. Phys. A: Math. Gen.* **20** 199–213
- [33] Knežević M and Vannimenus J 1987 Topological frustration and quazicompact phase in a model of interacting polymers *J. Phys. A: Math. Gen.* **20** L969–73
- [34] Kumar S and Singh Y 1990 Collapse transition of linear polymers on a family of truncated n-simplex lattices, *Phys. Rev.* **A42** 7151–54
- [35] Knežević D, Knežević M and Milošević S 1992 Critical behavior of an interacting polymer chain in a porous model system: Exact results for truncated simplex lattices 1992 *Phys. Rev. B* **45** 574–85
- [36] Živić I, Milošević S and Djordjević B 2005 On the total number of distinct self-interacting self-avoiding walks on three-dimensional fractal structures 2005 *J. Phys. A: Math. Gen.* **38** 555–65
- [37] Giacometti A and Maritan A 1992 Self-avoiding walks with curvature energy on fractals *J. Phys. A: Math. Gen.* **25** 2753–64
- [38] Tuthill G F and Schwalm W A 1992 Biased interacting self-avoiding walks on the four-simplex

- lattice *Phys.Rev. B* **46** 13722–34
- [39] Dhar D 1978 Self-avoiding random walks: Some exactly soluble cases *J. Math. Phys.* **19** 5–11
- [40] Dhar D 1977 Lattices of effectively nonintegral dimensionality *J. Math. Phys.* **18** 577–85
- [41] Rammal R, Toulouse G and Vannimenus J 1984 Self-avoiding walks on fractal spaces: exact results and Flory approximation *Journal de Physique* **45** 389–94
- [42] Polotsky A A and Ivanova A S 2021 On the adsorption of a polymer chain with positive or negative bending stiffness onto a planar surface *Physica A* **562** 125319
- [43] Živić I, Hadžić S E and Marčetić D 2022 Persistence length of semi-flexible polymer chains on Euclidean lattices *Physica A* **607** 128222
- [44] Elezović-Hadžić S, Marčetić D and Maletić S 2007 Scaling of Hamiltonian walks on fractal lattices *Phys. Rev. E* **76** 011107
- [45] Owczarek A L, Prellberg T and Brak R 1993 New scaling form for the collapsed polymer phase *Phys. Rev. Lett.* **70** 951–53
- [46] Prellberg T, Owczarek A L, Brak R and Guttmann A J 1993 Finite-length scaling of collapsing directed walks *Phys. Rev. E* **48** 2386–96
- [47] Duplatier B 1993 Exact Scaling Form for the Collapsed 2 D PolymerPhase *Phys. Rev. Lett.* **71** 4274
- [48] Baiesi M, Orlandini E and Stella A L 2005 Scaling of a Collapsed Polymer Globule in Two Dimensions *Phys. Rev. Lett.* **96** 040602
- [49] Guttmann A J, Jensen I and Owczarek A L 2022 Self-avoiding walks contained within a square *J. Phys. A: Math. Theor.* **55** 425201
- [50] Lekić D and Elezović-Hadžić S 2010 A model of compact polymers on a family of three-dimensional fractal lattices *J. Stat. Mech.* P02021
- [51] Marčetić D, Elezović-Hadžić S and Živić I 2021 Effects of the boundaries on the scaling form of Hamiltonian walks on fractal lattices *J. Phys.: Conf. Ser.* **1814** 012005
- [52] Owczarek A L and Prellberg T 2001 Scaling of self-avoiding walks in high dimensions *J. Phys. A: Math. Gen.* **34** 5773–80
- [53] Lekić D and Elezović-Hadžić S 2011 Semi-flexible compact polymers on fractal lattices *Physica A* **390** 1941–52
- [54] Marčetić D, Elezović-Hadžić S, Adžić N and Živić I 2019 Semi-flexible compact polymers in two dimensional nonhomogeneous confinement *J. Phys. A: Math. Theor.* **52** 125001